DIAGNOSTYKA, 2024, Vol. 25, No. 3

e-ISSN 2449-5220
DOI: 10.29354/diag/190318

FAILURE IDENTIFICATION AND ISOLATION OF DC-DC BOOST CONVERTER USING A SLIDING MODE CONTROLLER AND ADAPTIVE THRESHOLD

Fatma KHATER [1,*], Abderrezak AIBECHE [1], Sid Ali FELLAG [1], Mohamed Zinelabidine DOGHMANE [2], Hamza AKROUM [1]

[1] Laboratoire d'Automatique Appliquée (LAA), département d'automatisation et électrification des procédés, Faculté des hydrocarbures et de la chimie (FHC), Université M'hamed Bougara - Boumerdès, 35000, Algérie.
[2] Département Evaluation des Réservoirs, Direction des Opérations Exploration, Division Exploration, Sonatrach, Hassi Messaoud 30500, Ouergla, Algérie.
[*] Corresponding author, e-mail: f.khater@univ-boumerdes.dz

Abstract

DC-DC converters have become essential components in various industrial applications, including aerospace, electric vehicles, and renewable energy systems. However, ensuring enhanced reliability remains a critical challenge for these converters. Fault diagnosis and reliability analysis are crucial for preventing damage and minimizing maintenance costs. This study focuses on investigating the operational behavior of DC-DC boost converters under normal and faulty conditions, precisely targeting open-circuit and short-circuit faults in converter switches. To achieve this, an adaptive threshold approach is introduced for effective fault detection. The adaptive threshold value is calculated based on measured voltage and current signals, along with their corresponding reference signals from the primary control system. The research is structured into two parts: the first part addresses sliding mode control aspects, ensuring regulated output voltages, output currents, and capacitor voltage for sustained converter operation. The second part investigates fault diagnosis, analyzing the impact of defective DC-DC converters on the overall electrical system functionality. The proposed algorithm's performance is evaluated and validated through simulations in MATLAB/Simulink environment. Furthermore, based on the results' comparison, the proposed approach of the sliding mode controller and adaptive threshold contributes to enhancing the reliability of DC-DC converters and enables effective fault detection and isolation.

Keywords: DC-DC boost converter, faults detection and isolation, adaptive threshold, open-circuit and short-circuit faults, sliding mode controller, reliability analysis.

1. INTRODUCTION

DC-DC converters exhibit nonlinear characteristics due to their switching behavior, which poses a challenge for control design and robust stability analysis [1]. Boost-type DC-DC converters are commonly used in systems where the desired output voltage needs to exceed the input voltage [2]. However, controlling such converters is more complex compared to cases where the output voltage is lower than the input voltage. Several control methods, including Pulse Width Modulation (PWM) and open-loop control, have been extensively employed for decades due to their simplicity and ability to ensure converter's stability. Nevertheless, closed-loop control approaches, such as PI control, sliding mode controller (SMC), and fuzzy logic controller (FLC), have been developed to enhance stability and robustness [3-5].

The reliability of DC-DC converters is crucial since a single component failure can lead to system malfunction. Thus, fault diagnosis plays a vital role in fault-tolerant control strategies for these converters, primarily due to the high maintenance involved costs. Power semiconductor switches, particularly insulated gate bipolar transistors (IGBTs) and metal-oxide semiconductor field-effect transistors (MOSFETs), are highly susceptible to failure and account for over 30% of converter malfunctions. The most common types of power switch faults are open-circuit faults (OCF) and short-circuit faults (SCF) [6], [7]. From one hand, SCF is considered the most severe type of faults as it can cause significant damage and an immediate system shutdown. On the other hand, an OCF typically leads to partial or total loss of operation in one of the IGBTs within the static converter, resulting in performance degradation [8], [9]. Fault diagnosis methods can be broadly classified into two categories: signal-based methods and model-based methods. In this study, the monitored variables for fault diagnosis include output voltage and current.

Received 2023-10-09; Accepted 2024-06-21; Available online 2024-10-07

Fault diagnosis and fault-tolerant control strategies present significant challenges in enhancing system reliability, ensuring service continuity, and reducing maintenance costs, making them prominent areas of research in recent years [10], [11]. In [12], a fault detection method is introduced, it efficiently identifies switch faults in boost converters used in photovoltaic systems within one switching period. This method uses the sign of the inductor current slope as a diagnostic criterion, enabling the detection of both open-circuit faults (OCFs) and short-circuit faults (SCFs). After that, Chen et al., in [13] and [14] proposed another diagnosis method based on analyzing harmonic components of the magnetic near field in a DC-DC converter. Later on, Jamshidpour et al., in [15] and [16] presented methods capable of detecting and identifying OCFs and SCFs, which are crucial for fault isolation. These methods involve comparing the switch control value with the measured value of the inductor current slope in a DC-DC boost converter. While several methods have been employed for fault diagnosis, the aforementioned works focus on system-based approaches, which may result in significant delay and potentially catastrophic propagation of component failures. Furthermore, Diego et al., in [17] proposed a model-based fault detection and isolation (FDI) technique for boost DC-DC converters in photovoltaic (PV) maximum power point trackers (MPPTs), it addresses inefficiencies caused by open- and short-circuit faults while ensuring fast and reliable fault diagnosis through the use of a high-gain observer (HGO) and decoupling from PV current and load variations. Finally, Xu et al., in [18] proposed a fault-tolerant control method for an input-parallel-output-series (IPOS) converter, using an immersion and invariant observer (I and IO) for fault diagnosis and remedial action to detect and identify open-circuit switch failure within two switching periods, ensuring effectiveness, robustness, and rapidity of the method in simulations. The reliability of fault detection systems for OCFs and SCFs in DC-DC boost converters, as introduced in the two references [17] and [18], remains a subject of ongoing debate due to their direct impact on overall system performance. A high-performing converter is essential for efficient energy conversion, stable load voltage, and reliable power delivery, especially in applications requiring precise power regulation. Any degradation in converter performance can lead to inefficiencies, reduced system reliability, and potential malfunctions. Therefore, in this study, we investigate the behavior of the DC-DC boost converter and propose an adaptive threshold approach for fault diagnosis, ensuring reliable and rapid fault detection and addressing the abovementioned challenges.

The structure of the rest of the manuscript is organized as follows: In Section 2, we provide a concise model description of the DC-DC boost converter. Section 3 elaborates on the control aspects of the converter, including a comparative analysis of its performance under open-loop and closed-loop control using a sliding mode controller compared to a PI controller. In Section 4, we focus on investigating faults in the converter, more precisely the diagnosis of open-circuit (OC) and short-circuit (SC) faults. This section examines the behavior of the converter under faulty conditions, explores the impacts of these faults on the electrical system, and verifies the effectiveness and reliability of the proposed adaptive threshold for fault identification and isolation. The study is concluded with a summary of the key findings and recommendations for future work.

2. DC-DC BOOST CONVERTER MODEL

DC-DC converters are electronic devices used to modify DC output voltage levels. DC-DC boost converters are electronic circuits used to step up voltage levels from a lower input voltage to a higher output voltage. They are essential in various applications where a higher voltage is required. Boost converters are highly efficient and are available in various configurations to suit different power requirements and design constraints. They play a crucial role in modern electronics, enabling the efficient use of power sources and the generation of high voltages from low-voltage inputs.

The DC-DC boost converter comprises essential components such as a MOSFET or IGBT transistor, a diode, a capacitor, an inductor, and a control circuit responsible for regulating the MOSFET gate using a pulse width modulation (PWM) signal [19]. The operation of the DC-DC converter can be divided into two distinct phases. In the first phase, known as the "on-state" phase, the IGBT is active, allowing the source voltage to supply the load while simultaneously charging the inductor and capacitor. The second phase begins when the IGBT is switched off. During this "off-state" phase, the load is powered by the discharge of the inductor and capacitor. The boost circuit is designed to convert the input voltage (E) to an output voltage (Vload), where Vload is greater than E (Fig. 1). To obtain the mathematical model of the DC-DC boost converter, we apply Kirchhoff's laws to the circuit depicted in Fig. 1, considering the operating regime and the condition of the switch (S). The obtained model is given by equation (1).

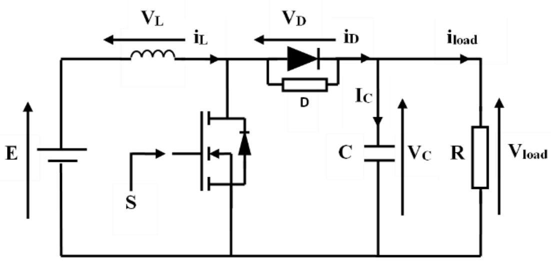

Fig. 1. Diagram of the studied DC-DC boost converter

$$\begin{cases} L\frac{di_L}{dt} = E \\ C\frac{dV_C}{dt} = -\frac{V_C}{R} \end{cases} \quad (1)$$

During the on-state of the power switch, when it is closed, current flows from the input source through the inductor, leading to the accumulation of energy in the inductor's magnetic field. The diode, in this period, remains reverse-biased and does not conduct. Then, during the off-state of the power switch, when it is opened, the inductor releases the stored energy. As a result, the diode becomes forward-biased, allowing the flow of current through it. The current from the inductor continues to flow through the diode, charging the capacitor and simultaneously delivering power to the load. When the switch SW is closed, D is blocked on the t_{on}, where $t_{on} = \alpha \times T$. When the switch SW is opened, D is ON, on the period t_{off}, where $t_{off} = (1 - \alpha) \times T$. The equation in the ON state is given by (2).

$$\begin{cases} L\frac{di_L}{dt} = E - V_C \\ C\frac{dV_C}{dt} = i_L - \frac{V_C}{R} \end{cases} \quad (2)$$

The general average model that defines the boost converter operation is given by equation (3).

$$\begin{cases} L\frac{di_L}{dt} = E - (1-\alpha)V_C \\ C\frac{dV_C}{dt} = (1-\alpha)i_L - \frac{V_C}{R} \end{cases} \quad (3)$$

Let $x_1 = i_L$ and $x_2 = V_C$. Then, equation (3) is transformed into the state space representation $\dot{x} = Ax + Bu$ given by equation (4).

$$\begin{bmatrix} \dot{x}_1 \\ \dot{x}_2 \end{bmatrix} = \begin{bmatrix} 0 & -(1-u)\frac{1}{L} \\ (1-u)\frac{1}{C} & -\frac{1}{RC} \end{bmatrix} \begin{bmatrix} x_1 \\ x_2 \end{bmatrix} + \begin{bmatrix} \frac{1}{L} \\ 0 \end{bmatrix} E \quad (4)$$

The dynamic equations governing the behavior of this converter are derived based on the continuous conduction state, taking into account the current in the inductor (i_L) and the voltage across the capacitor (V_{load}) as previously discussed in [4] and [20]. The system parameters are defined as follows: the inductance of the coil (L) measured in Henrys (H), the capacitance of the capacitor (C) measured in Farads (F), and the load modeled as a resistor (R) measured in $Ohms$ (Ω). The state variables of the system are the current flowing through the coil and the voltage across the capacitor. The control signal (u) in the discrete domain $\{0, 1\}$, represents the state of the switch (S): 0 for open and 1 for closed. It can be replaced by its average value over a switching period (α), which indicates the duty cycle.

3. DC-DC BOOST CONVERTER CONTROL

Thorough analysis, control, and stabilization are essential factors in switch converters. Effective control of power converters is crucial to provide the load with the required voltage, current, and frequency while ensuring desired system dynamics. Numerous control approaches have been developed and documented in the literature for switch-mode DC-DC converters. In many industrial and high-performance applications, a straightforward and cost-effective controller structure is highly desirable. One commonly used control technique is Pulse Width Modulation (PWM), which is a simple open-loop control method that guarantees stability for the studied converter. However, for applications requiring enhanced dynamics, various closed-loop control strategies have been developed and implemented along with a PWM modulator (Fig. 2). These include PID controllers, fuzzy logic control (FLC), and sliding mode controllers. Each control method has its own advantages and limitations, which determine its suitability under specific conditions compared to other control techniques. However, there is a continuous demand for a control method that consistently delivers superior performance across diverse operating conditions.

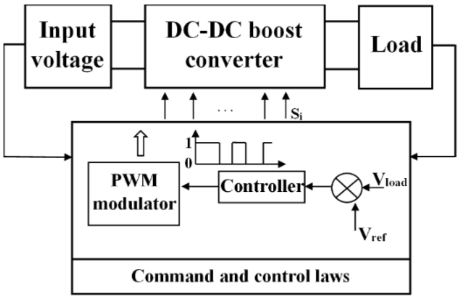

Fig. 2. General scheme of DC-DC boost converter control with PWM.

In this part of the study, the control of the converter operates in an open-loop configuration, indicating the absence of feedback to regulate the system's state variables. In this context, we have employed the PWM-ST (Pulse Width Modulation with Sine-Triangle) technique as an open-loop control approach [21], [22]. The fundamental principle of this strategy involves comparing a reference or modulating sinusoidal signal $m(t)$ with a higher-frequency carrier signal $p(t)$, as shown in Fig. 3. This comparison enables the generation of a PWM signal that serves as a switching function to control the converter's switches.

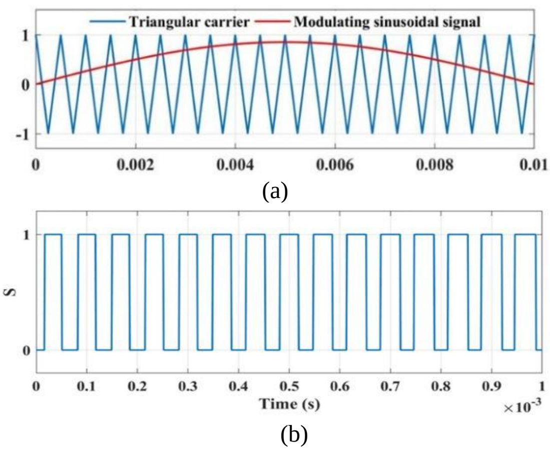

(a)

(b)

Fig. 3. Principle of the PWM control: (a) $m(t)$ with $p(t)$, (b) State of the Switch (S)

3.1. PI control design

The primary objective of the PID control law is to regulate the output voltage and current of the system. The PID controller, which belongs to the family of classical control techniques, finds widespread use in DC-DC converters [2]. Within this controller family, various combinations of proportional (P), integral (I), derivative (D), the PID controllers offer multiple approaches for controlling the DC power supply in these converters [23], [24].

The PID controllers are commonly employed in industrial applications within the field of power electronic converters, owing to their numerous advantages. The simplicity of tuning methods, such as the Ziegler-Nichols tuning method, facilitates easy optimization of the proportional, integral, and derivative terms of this control technique to achieve the desired closed-loop performance. This attribute contributes to the continued employment of this classical technique in industrial applications. The conventional PID regulator establishes a direct relationship between the control signal $u(t)$ and the error signal $e(t) = V_{load} - V_{ref}$, as described by equation (5).

$$U(t) = K_p(e(t) + \frac{1}{T_i}\int e(t)dt + T_d\frac{de(t)}{dt} \quad (5)$$

In order to avoid singularities that might be generated by the discontinuities in the derivative term in equation (5), the PI control technique is a commonly used approach in electrical energy conversion systems. This regulator is built upon the determination of the output, denoted as U, which is influenced by the proportional gain (K_p) and integral gain (K_I) parameters as given in equation (6). These gains represent the specific contributions of the proportional and integral actions of the regulator shown in Fig. 4. It should be emphasized that the values of K_p and K_I may exhibit variability depending on the operating conditions of the system.

$$U(t) = K_p e(t) + K_I \int e(t)dt \quad (6)$$

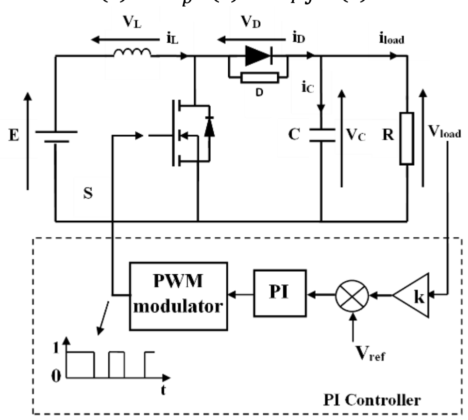

Fig. 4. Diagram of the DC-DC boost converter regulated by PI controller.

3.2. Sliding mode control

Sliding mode control, originally introduced for the control of variable structure systems [25], is a nonlinear control technique. The methodology of sliding modes involves directing the trajectory of the system's state towards a designated sliding surface and using switching logic to maintain it in close proximity to this surface until reaching the equilibrium point. Sliding mode control is a robust control approach that relies on the concept of the controller structure adapting to the system's state to achieve the desired response. The resulting control from sliding mode, in this study, is of a binary nature, with an "on-off" characteristic [20]. This control principle is primarily based on the use of a discontinuous control signal, aimed at guiding the system's evolution along a carefully selected switching sliding surface [26]. Thus, the synthesis process aims to establish the attractiveness condition of the sliding surface, ensuring its attraction from any point within the state space [27]. Once the sliding surface is reached, it becomes crucial to ensure sliding along this surface, satisfying the sliding condition, and guaranteeing the stability of the system, as determined by the stability condition. This principle of stability is established by considering the Lyapunov criterion as the foundation for stability assessment [28]. For the state space representation in equation (4), let us consider the positive Lyapunov function V, defined as follows:

$$V(S) = \frac{1}{2}S^2 \quad (7)$$

The sliding surface is defined by:

$$S = x_1 - x_{1ref} \quad (8)$$

The first derivative of the sliding surface is obtained as:

$$\dot{S} = i_L - i_{L\_ref} \quad (9)$$

By replacing equation (3) in equation (9), we obtain:

$$\dot{S} = -\frac{(1-u)}{L}V_{load} + \frac{E}{L} - i_{L\_ref} \quad (10)$$

By using the first derivative of the Lyapunov function in equation (7), and replacing equation (10), the necessary condition to guarantee the system stability is obtained as follows:

$$\dot{V} = S \cdot \dot{S} = S \cdot \left[-\frac{(1-u)}{L}V_{load} + \frac{E}{L} - i_{L_{ref}}\right] < 0 \quad (11)$$

The sliding mode controller necessary to achieve finite-time convergence to the sliding surface is defined as follows:

$$u = \begin{cases} 1 & if\ S > 0 \\ 0 & if\ S < 0 \end{cases} \quad (12)$$

The corresponding control law for the DC-DC boost converter is formulated as follows:

$$u = \frac{1}{2}\left(1 + sign(S)\right) \quad (13)$$

It has been supposed that the discontinuity at $S = 0$ do not occur often for such systems. The choice of the control input in equation (12) guaranteed the negative definitiveness of equation (11), consequently, the Lyapunov stability of DC-DC system with SMC. The implementation of the sliding mode controller designed for the DC-DC boost converter is depicted in Fig. 5.

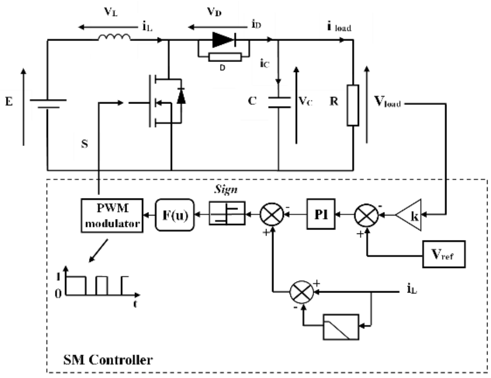

Fig. 5. Control scheme of the DC-DC boost converter by Sliding Mode Controller (SMC)

3.3. Healthy operating mode simulations

In this section, the DC-DC boost converter circuit is simulated under a MATLAB/Simulink 2018a environment using the parameters' values summarized in Table 1. The values for voltage, resistance, and other parameters in simulation tests for DC-DC converters can vary depending on the specific design and intended application of the converter. Resistance values are pivotal in DC-DC boost converter simulations, particularly the load resistance Rch, which represents the resistance of the converter at its output terminals. Often, we choose this value based on the load we intend the converter to control, which can vary significantly depending on the application. Proper selection of these values is essential to ensuring stable and reliable operation.
Input Voltage (Vin): This refers to the voltage supplied to the DC-DC converter; this can vary significantly depending on the application of this converter. Common ranges might be from a few volts to hundreds of volts for some industrial applications.
Output Voltage (Vout): This represents the DC converter's intended voltage output, tailored to specific application requirements.
Switching Frequency: This is the frequency at which the DC-DC converter switches on and off. Common frequencies typically range from kilohertz to several megahertz.
Switching Duty Cycle: This refers to the ratio of the on-time to the total switching period of the converter. It's usually expressed as a percentage and can vary depending on the converter's design and operating conditions.

Table 1. Operating parameters of the studied DC-DC boost converter

Parameter	Description	Values
Vin [V]	Input DC voltage	2500
α [%]	The duty cycle	40
L [H]	Inductor	2.5×10^{-3}
R [Ω]	Resistor	10^{-2}
C [F]	Capacitor	10^{-5}
Rch [Ω]	Load resistance	50
Lch [H]	Load inductance	10^{-3}
f_{PWM} [kHz]	The switching frequency	5
Te [sec]	The switching period	10^{-6}

During healthy normal operation, the PI and SMC controllers discussed earlier are applied to control the DC-DC boost converter, followed by a comparative analysis of their respective performances. Initially, Pulse Width Modulation (PWM), also known as natural control, is employed for open-loop control of the DC-DC boost converter. PWM is selected for its simplicity and practicality, allowing manipulation of the duty cycle of the switching signal. After that, closed-loop control is implemented using the proposed controllers. The effectiveness of each control strategy is assessed, and the most suitable approach for controlling the DC-DC boost converter in the system is determined through a comprehensive comparison and evaluation of their stability, accuracy, and robustness in both open and closed loop scenarios.

Based on Fig. 6, the open-loop control of the converter using the PWM technique demonstrates its effectiveness in terms of stability and ease of implementation. However, it exhibits significant peak amplitudes during transient states, and considerable fluctuations in the load voltage curve (Fig. 6a) and the load current curve (Fig. 6b). Nevertheless, in applications requiring higher dynamics, the precision and sensitivity of the open-loop controlled DC-DC converters may prove insufficient, particularly when encountering changes in the operating conditions.

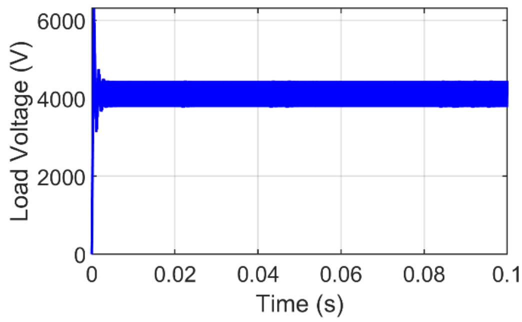

(a)

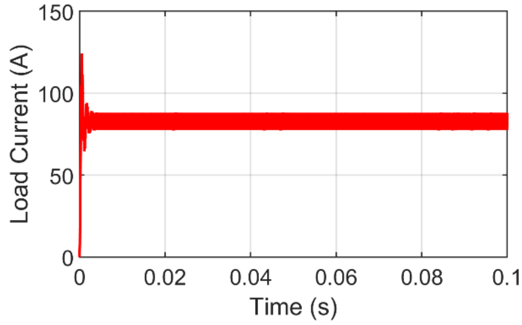

(b)

Fig. 6. Open-loop responses of DC-DC converter based on PWM for: a) Load voltage, b) Load current

To address this limitation, closed-loop control is employed to enhance the dynamic behavior of the converter, enabling control of relevant quantities despite operational variations. Figures 7 and 8 illustrate the response of the output variables of the

DC-DC boost converter under closed-loop control, using the PI and SMC controllers, respectively.

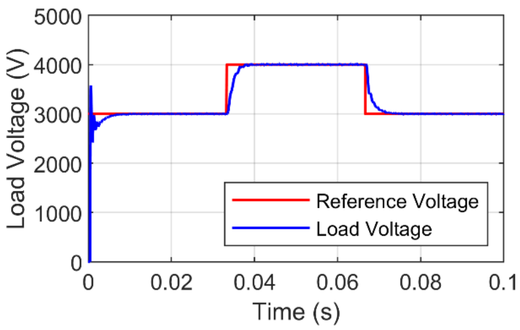

(a)

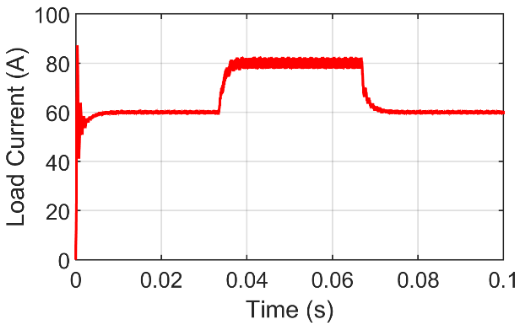

(b)

Fig. 7. Closed-loop responses of the DC-DC converter controlled by PI for: a) Load voltage, b) Load current

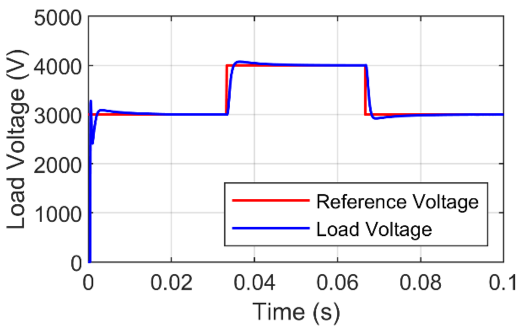

(a)

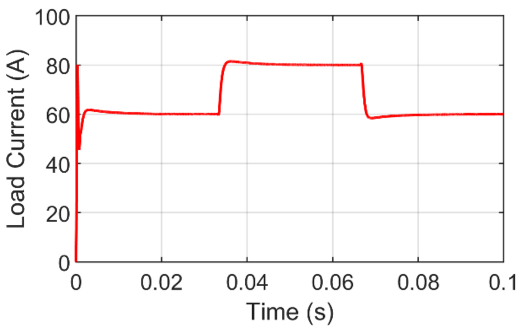

(b)

Fig. 8. Closed-loop responses of the DC-DC converter controlled by SMC for: a) Load voltage, b) Load current

To assess the robustness of the converter against input voltage fluctuations, its behavior is tested under varying input voltage conditions. Remarkably, the output variables closely tracked their respective reference values, displaying minimal static error. More preocisely, the load voltage controlled by the PI (Fig. 7a) showed more fluctuation and static error than the load voltage controlled by the SMC (Fig. 8a). Moreover, the load current obtained by PI (Fig. 7b) exhibited more fluctuations and static error than the load current obtained by the SMC (Fig. 8b). Upon analyzing the fluctuations in the preceding curves, it is evident that the output voltage effectively tracks its reference value despite the input voltage variations for both controllers. However, the implementation of the SMC has demonstrated improved tracking performance, illustrating its suitability for meeting stability and robustness requirements. Furthermore, this control method has led to reduced static errors and overshoots while enhancing the overall response time under healthy mode, thus it will be tested in faulty operating conditions.

4. DC-DC POWER CONVERTER FAULTS

Enhancing the reliability of DC-DC converters is a critical aspect of ensuring uninterrupted service in various industrial applications [29]. Therefore, extensive research has been conducted to address fault diagnosis and reliability analysis of static converters, aiming to prevent converter damage, production loss, and minimize maintenance costs. Failures in power converters can arise from various components, such as capacitors, power devices, gate drivers, inductors, resistors, and others. Among these, capacitor degradation represents a significant reliability concern in switching-mode power converters. Furthermore, variations in the converter's voltage response serve as valuable indicators of its faulty state. Nevertheless, semiconductor switch faults remain the most prevalent type of fault in converters [30], [31], [32]. This can be attributed to the delicate nature of semiconductor switches, which are highly susceptible components in power converters. This section addresses both OCF and SCF. Failure to diagnose and protect against these faults can result in complete failures of other switches and circuit components.

4.1. Faults diagnosis based on sliding mode

The primary objective of fault diagnosis is to promptly detect and identify various types of failures at their early stages, enabling timely shutdown and the planning of maintenance actions. A fault diagnosis system typically performs three essential tasks, as indicated in the literature [33], [34]:

- Fault detection: This involves determining whether a fault has occurred or not by analyzing signals and detecting deviations from expected behavior.
- Fault identification: Once a fault is detected, the fault identification task aims to generate signals or indicators that can determine the type of fault that has occurred and identify the specific faulty component or switch.

- Fault isolation: After identifying the faulty component, the fault isolation task focuses on isolating the faulty component from the rest of the circuit to prevent further damage to the system. This may involve disabling or bypassing the faulty component while allowing the rest of the system to continue functioning.

Based on this analysis, we will investigate the impacts of faults applied at time t=0.05 s to the DC-DC boost converter. More precisely, we will examine the effects of an open-circuit fault (OCF) and a short-circuit fault (SCF) on the DC-DC converter dynamic. Figures (9) and (10) depict, respectively, the dynamics of the output voltages and currents of the DC-DC boost converter in the presence of faults, specifically an OC fault and a SC fault on the IGBT. While an OC fault in the converter leads to a drop in performance (Fig. 9a and Fig. 9b), it does not immediately result in a system failure. In this scenario, it has been noticed that the appearance of OCF has led to a considerable drop in load voltage (Fig. 9a) and load current (Fig. 9b). On the other hand, SC faults in power switches present significant challenges due to the exposure of the damaged component to high current, high voltage, and elevated local temperatures. As noticed in Fig. 10, the appearance of SCF has led to a complete loss of load voltage (Fig. 10a) and load current (Fig. 10b). It is crucial to carefully study the impact of faults in terms of system robustness and availability in degraded mode. If a fault is not detected and compensated in real-time, it can propagate and result in additional faults in the energy conversion chain's functional blocks. For power converters, it is desirable to detect, identify, diagnose, and protect against various fault types. The results obtained from this scenario highlight the critical importance of employing a robust fault detection and isolation approach for DC-DC converters.

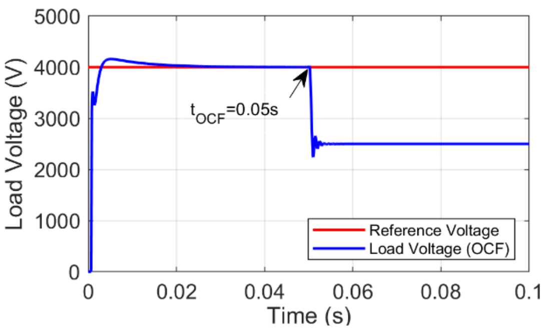

(a)

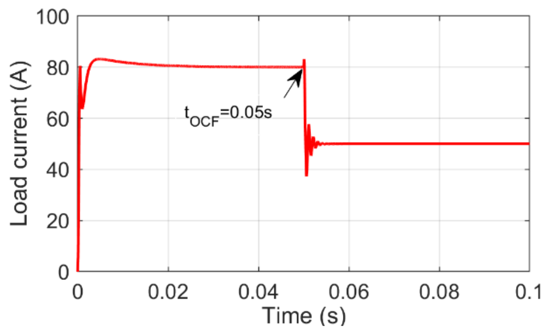

(b)

Fig. 9. The DC-DC converter responses with the appearance of OCF for: a) Load voltage, b) Load current

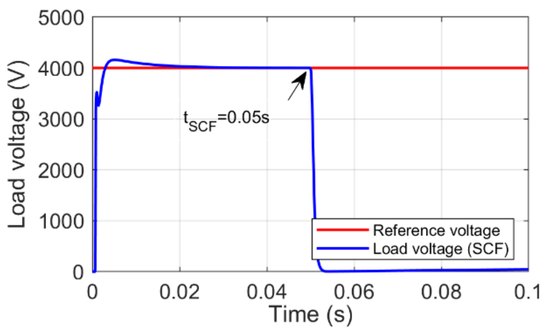

(a)

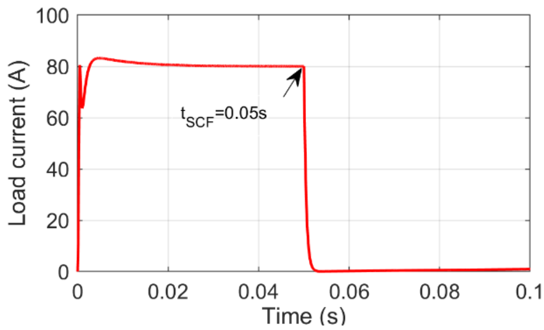

(b)

Fig. 10. The DC-DC converter responses with the appearance of SCF for: a) Load voltage, b) Load current

The system is primarily used for SCFs due to their significant impact on the overall system. Moreover, the algorithm is applied to compensate for OSFs. Therefore, the basic principle of fault diagnosis methods used in this study for the DC-DC boost converter is proposed and illustrated in Fig. 11. Moreover, the detailed flowchart of the proposed method for fault detection, identification, and isolation is given in Fig. 12.

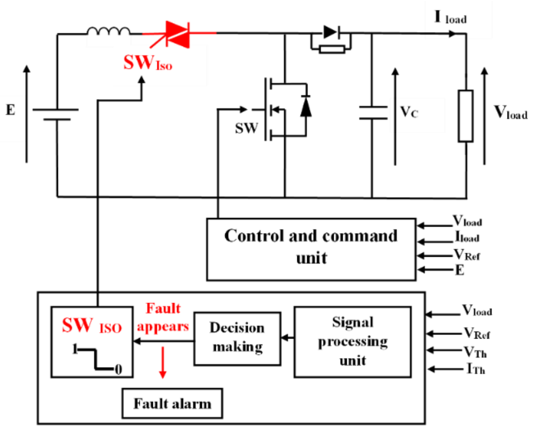

Fig. 11. General diagram of fault diagnostic for DC-DC boost converter

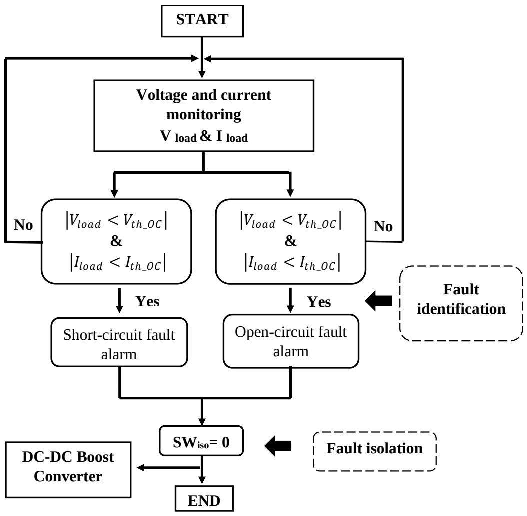

Fig. 12. Detailed flowchart of fault diagnostic for DC-DC boost converter

4.2. Faults detection and identification

The detection and identification of OC and SC faults in DC-DC boost converters play a vital role in ensuring the safe and reliable operation of power electric systems. This process typically involves the monitoring and analysis of various electrical parameters. In this part of the study, the technique employed for fault detection and identification is voltage and current monitoring. By observing the signals of voltage and current, valuable insights into the converter's operation can be obtained. Sudden changes or anomalies in these signals can serve as indicators of a fault. Current and voltage sensors are commonly employed for this purpose in other types of converters. In the case of an OC fault occurring at time T_1 in the IGBT, the degraded operating condition is characterized by significant distortions in the load voltage and current, as depicted in Fig. 9. These deformations result in a notable decrease in the steady-state values of the voltage and charging current. On the other hand, in the event of an SC fault (Fig. 10), an abrupt decline in both voltage and load current occurs immediately.

To detect significant deviations between the measured voltage and current under faulty conditions, voltage and current threshold values have been set (V_{th} and I_{th}). These threshold values serve as reference points against which the measured values are compared. When a fault occurs, the measured voltage and current may deviate significantly from their expected values. By appropriately selecting threshold values, a range can be defined within which the measured values are considered normal. If the measured values exceed or fall below these threshold values, it indicates a potential fault condition, as detailed in Definition 1.

- Definition 1: The faults detection and identification method is based on the following assumption:

  If $|V_{load} < V_{Th\_OC}|$ and $|I_{load} < I_{Th\_OC}|$, then the fault is assumed to be OC switch fault.

  If $|V_{load} < V_{Th\_SC}|$, and $|I_{load} < I_{Th\_SC}|$, then the fault is assumed to be SC switch fault.

V_{load}: load voltage, is the voltage at the output terminals of the DC-DC converter; it is the voltage supplied to the load.
V_{ref}: reference voltage is a stable voltage level used as a point of comparison against which other voltages are controlled in the converter
I_{load}: load current, is the current flowing through the load connected to the output of the DC-DC converter.
I_{in}: initial current refers to the current that flows when the converter is first activated.
V_{Th_OC} and I_{Th_OC}: voltage and current threshold values for an OC fault. This is the maximum allowable outputs voltage and current that the converter can deliver without triggering the OC fault.
V_{Th_SC} and I_{Th_SC}: Voltage and Current threshold values for an SC fault. This denotes the maximum permissible outputs voltage and current that the converter can supply without activating the SC fault.

- Threshold selection analysis

The threshold values play a crucial role in the domain of fault diagnosis. The selection of appropriate threshold values depends on the studied system and the desired sensitivity to fault detection. It is imperative to choose values that reflect a significant deviation from normal operation while minimizing false alarms. These threshold values can be determined through analysis and simulation, taking into account the anticipated behavior of the system in various failure scenarios. By establishing suitable threshold values, abnormal voltage and current measurements can be effectively identified and flagged, enabling the timely detection and diagnosis of faults in the system. In this study, careful selection of threshold values is of paramount importance. The proposed threshold values for voltage and current are defined in equations (14) and (15), respectively.

$$V_{Th} = \mu \cdot V_{ref} + \alpha \cdot \frac{V_{load}}{V_{ref}} - 1 \qquad (14)$$

$$I_{Th} = \mu \cdot I_{in} + \alpha \cdot \frac{I_{load}}{I_{in}} - 1 \qquad (15)$$

Where μ is a constant used to designate the type of fault; it can take two values: μ_{OC} for the OCF and μ_{SC} for the SCF. α is given by (16).

$$\alpha = 1 - \frac{V_{ref}}{V_{Load}} \qquad (16)$$

The effectiveness and robustness of the proposed threshold values in equations (14) and (15) depend on the reference voltage and load voltage, making them susceptible to false alarms in the presence of disturbances. To validate the performance of the proposed threshold under varying input voltage and load disturbances, a series of simulation tests has been conducted. Initially, variations in the input voltage are introduced at $T_1 = 0.03$ s and $T_2 = 0.07$ s, respectively.

Figure 13a and Fig. 14a illustrate the adaptation of the threshold voltage and current to these voltage variations. It can be observed that the threshold values are adjusted accordingly as the input voltage transitions from one level to another. After that, disturbances are applied to the charge values, resulting in a 50% increase in their magnitude. As depicted in Figs. 13b and 14b, the threshold values exhibit a similar response, tracking the variation in the load voltage and current, respectively.

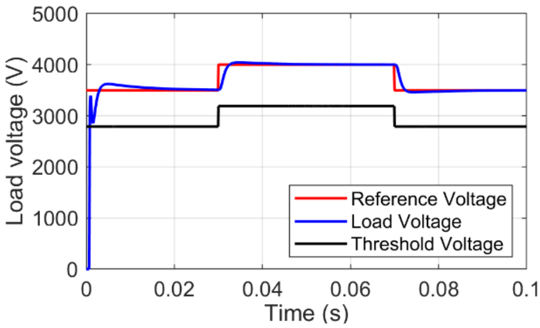

(a)

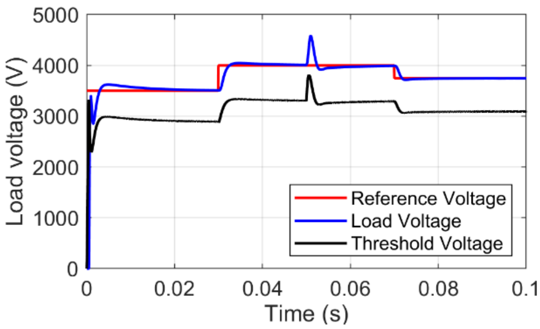

(b)

Fig. 13. The threshold voltage responses under: (a) Reference voltage variation, (b) Charge disturbance

These results indicate that the selected threshold is effective in the presence of input voltage and load disturbances. Hence, through these simulations, it is evident that the proposed threshold demonstrates effectiveness and resilience in the face of disturbances in both the input voltage and the load conditions. Therefore, the performance of the proposed approach in isolating both OCF and SCF will be discussed in detail in the next subset of simulation scenarios.

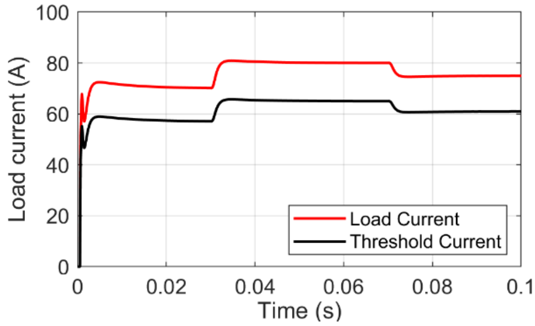

(a)

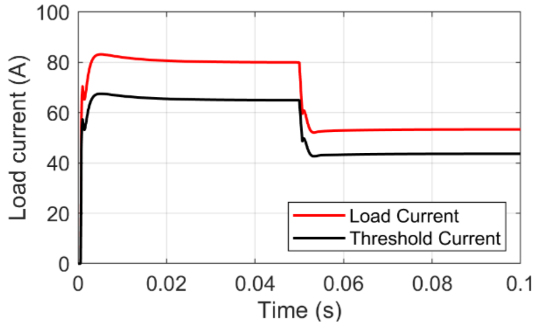

(b)

Fig. 14. The threshold current responses under: (a) Reference voltage variation, (b) Charge disturbance

4.3. Faults isolation

In the fault detection stage, a fault alarm is triggered to indicate the presence of a fault without providing information about the specific faulty component or the fault mode. Thence, during the fault identification phase, the faulty component and the type of fault that caused the alarm should be determined. This combined process of fault detection and fault identification is commonly known as "fault diagnosis", which aims to determine the nature, location, and type of the fault. As mentioned before, the occurrence of defects in the system is typically characterized by a significant decrease in the output voltage and current, as demonstrated in Figs. (9) and (10). Therefore, it is crucial to take effective actions upon detecting and identifying specific faults. The subsequent step, fault isolation, involves the utilization of hardware redundancy design and fault-tolerant control strategies. Fault isolation, detailed in definition 2, is implemented to separate the faulty components and reconfigure the converter to ensure safe and uninterrupted operation.

- Definition 2: The faults' isolation method is based on the following assumption:
  The switch is set to T_i , which is the time at which the fault is detected, then the isolation switch (SW_{iso}), should be changed from 1 to 0 for both the OCFs and SCFs as given by equation (17).

$$\begin{cases} SW_{iso} = 1, & fault-free\ operation \\ SW_{iso} = 0, & Operation\ with\ defects \end{cases} \quad (17)$$

4.4. Simulations results of faults diagnosis

A comprehensive set of simulation tests is conducted to assess the performance of the proposed fault diagnosis method. During the fault detection and identification phase, the fulfilment of the conditions given in Definition 1 signifies the presence of either an OC or SC faults. Depending on the precise moment at which the faults occur, our proposed algorithm can promptly detect and accurately identify the specific fault type.

Figures (15) and (16) present the voltage and current signals of switch faults in the DC-DC boost converter when OC and SC faults occur at T=0.05 s.

Fig. 15a demonstrates the effectiveness of the proposed algorithm in detecting the OC fault from the load voltage signal, while Fig. 15c provides a zoomed view around the fault time $T = 0.05$ s. Similarly, Fig. 15b shows the identification of the OC fault based on the load current signal, with Fig. 15d providing a zoomed view around $T = 0.05$ s. The results clearly demonstrate the success of the proposed algorithm in detecting and identifying switch faults during an OC fault. However, considering the importance and criticality of SC faults in DC-DC boost converters, it is imperative to ensure the reliability of the approach for SCF detection as well. Fig. 16a shows the results of detection and identification of the load voltage under SCF, with Fig. 16c offering a zoom around the fault time T = 0.05 sec. The algorithm effectively detects and identifies SC faults in real-time based on the load voltage signal. Similarly, Fig. 16b illustrates the identification of SCF based on the load current signal, and Fig. 16d presents a zoom around the SC fault time. The obtained results confirm that the proposed approach is capable of detecting and identifying both OC and SC faults in the DC-DC converter. Moreover, Table 2 provides precise instants at which the detection of faults occurred. It is also essential to discuss the effectiveness of our proposed approach in isolating the detected OC and SC faults to maintain the good performance of the DC-DC converters and protect the global system.

Table 2. Detection and identification instants for OCF and SCF

	μ	Tfault (s)	Tdet, Vch(s)	Tdet, Ich(s)
OCF	μ_{OC}=0.8	0.05	0.05026	0.05029
SCF	μ_{SC}=0.5	0.05	0.05033	0.05034

The fault diagnosis method investigated in this study is primarily designed to operate effectively in the presence of OCFs and SCFs occurring in the power switch. However, the efficiency of this method in isolating these faults should be investigated, as discussed in the subsequent scenario.

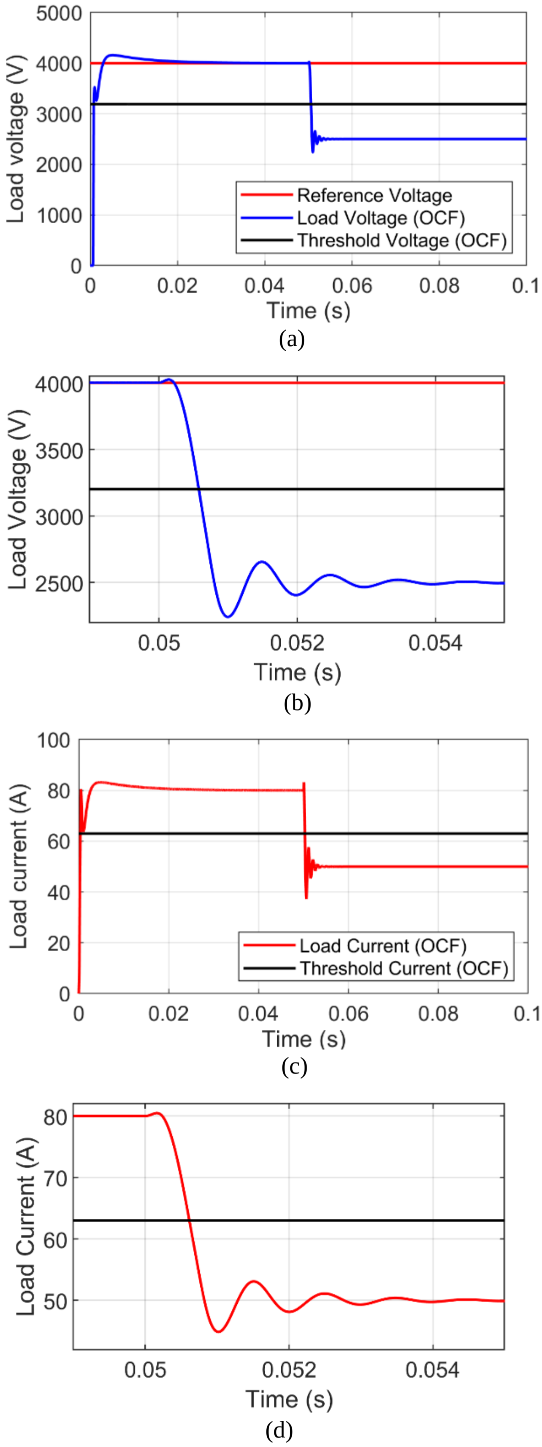

Fig. 15. Detection and identification of OCF (a) Load voltage monitoring, (b) Zoom of (a), c) Load current monitoring, d) Zoom of (c)

Upon fault detection, the diagnosis method enters fault isolation mode, where a common post-fault reconfiguration action is initiated regardless of the fault type. Precisely, the switch S_{iso} undergoes an update, transitioning from 1 (representing normal operation) to 0 (indicating fault isolation). This activation of the fault isolation mechanism ensures the segregation of the faulty component from the rest of the DC-DC boost converter system.

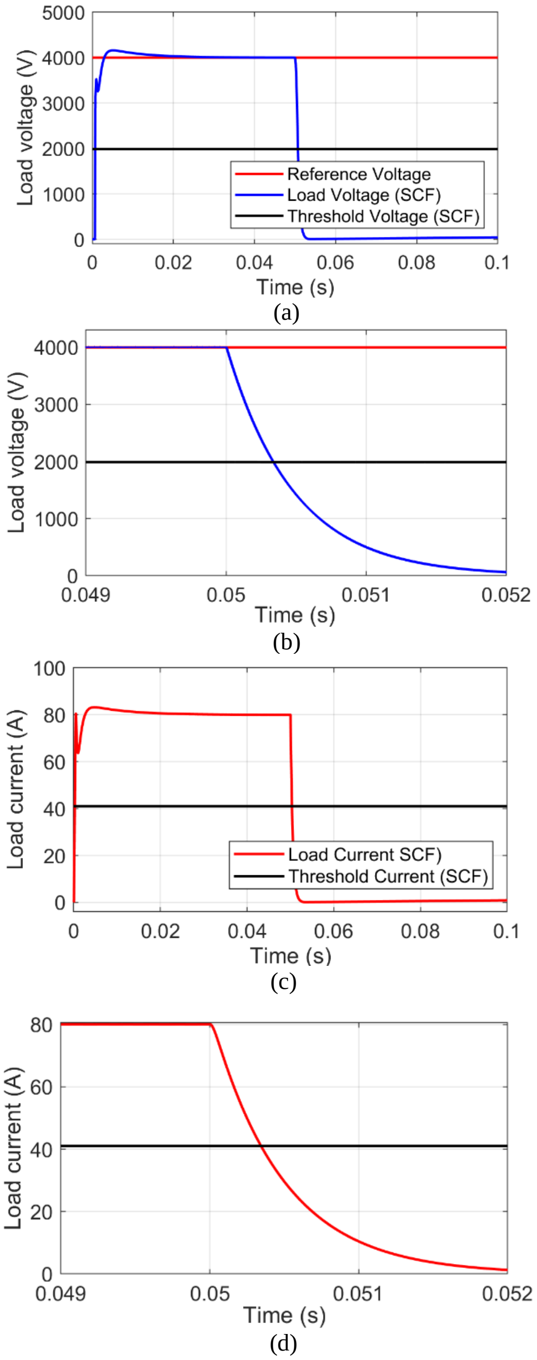

Fig. 16. Detection and identification of SCF: a) Load voltage monitoring, b) Zoom of (a), c) Load current monitoring, d) Zoom of (c)

Thereby preventing adverse effects on overall system operation and minimizing the risk of further damage or malfunction. The updating of S_{iso} is a critical step of the fault detection and isolation process, contributing to the system's ability to effectively manage and address identified faults while maintaining the integrity and dependability of its operation.

To validate the effectiveness of the proposed post-fault reconfiguration method, a simulation test is conducted for both OC and SC faults, as illustrated in Fig. 17. The fault occurs at $t = 0.05\ s$, and upon fault detection, the algorithm transitions into the fault isolation mode, adjusting the switching of S_{iso} according to definition 2. Fig. 17a$_1$ shows the real-time activation of the switch isolation to protect the system from OCF, and the load current shown in Fig. 17a$_2$ confirms this observation. Moreover, the SCF is successfully isolated based on the load voltage signal, as shown in Fig. 17b$_1$, and this is further confirmed by the load current under SCF in Fig. 17b$_2$. As a result, the faulty switch is effectively isolated, safeguarding the converter from potential harm.

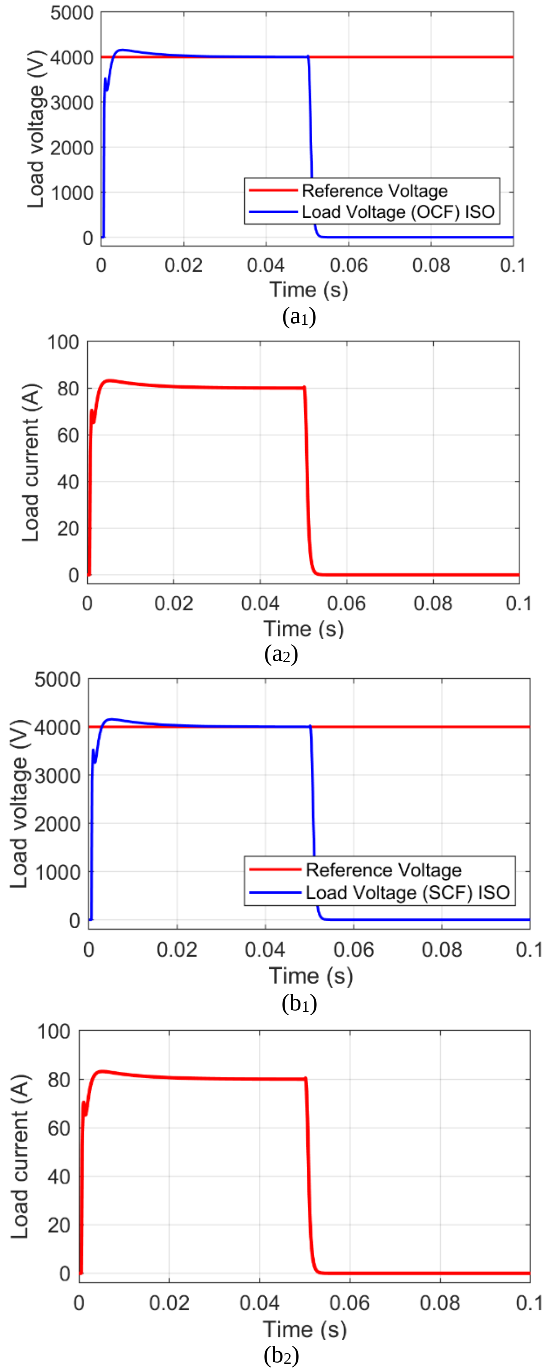

Fig. 17. Isolation phase of: a$_1$) Load voltage in OCF, a$_2$) Load current in OCF, b$_1$) Load voltage in SCF, b$_2$) Load current in SCF

Figures (17) and (18) illustrate the isolation phase of OC and SC faults. Where Fig. 18 shows a zoom of the obtained results around the isolation time, Fig. 18a demonstrates the OCF results of the load voltage curve, while Fig. 18b is dedicated to the load current curve of the DC-DC converter. Furthermore, Table 3 summarizes the precise instants at which the detection and isolation of OC and SC faults occurred.

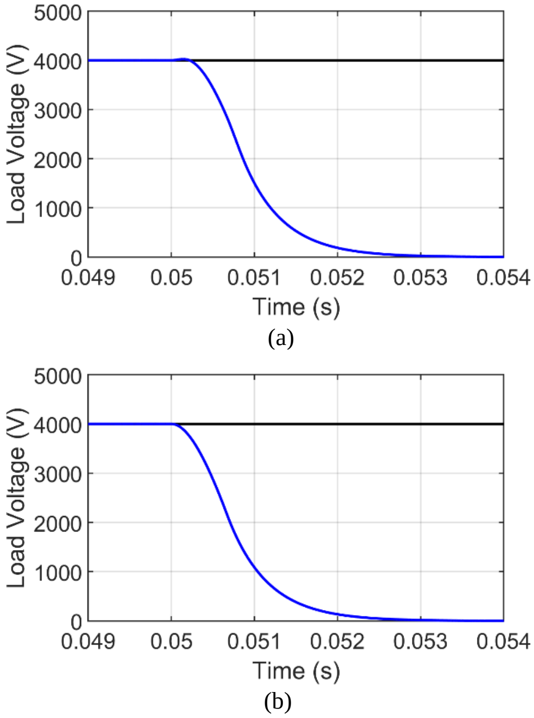

Fig. 18. Zoom of the isolation phase of: a) Load voltage in OCF, b) Load voltage in SCF

Table 3. Detection and isolation instants for OCF and SCF

	Tfault (s)	ΔTdet(s)	ΔTIso (s)
OCF	0.05	0.00026	0.003
SCF	0.05	0.00033	0.003

Moreover, Fig. 19 presents the precise time instances at which occurrences of open-circuit faults (OCFs) and short-circuit faults (SCFs) are observed, along with the corresponding fault detection and fault isolation events.

Whereas Fig. 19a$_1$ illustrates the appearance of OCF, Fig. 19a$_2$ indicates the OC fault detection time, and Fig. 19a$_3$ displays the OCF isolation time. Similarly, Fig. 19b$_1$ depicts the appearance time of SCF, Fig. 19b$_2$ shows the SCF detection time, and Fig. 19b$_3$ demonstrates the SCF isolation time. Upon analyzing these times, it is evident that the time between detection and isolation is minimal for both OCF and SCF, validating the reliable and efficient nature of the proposed approach.

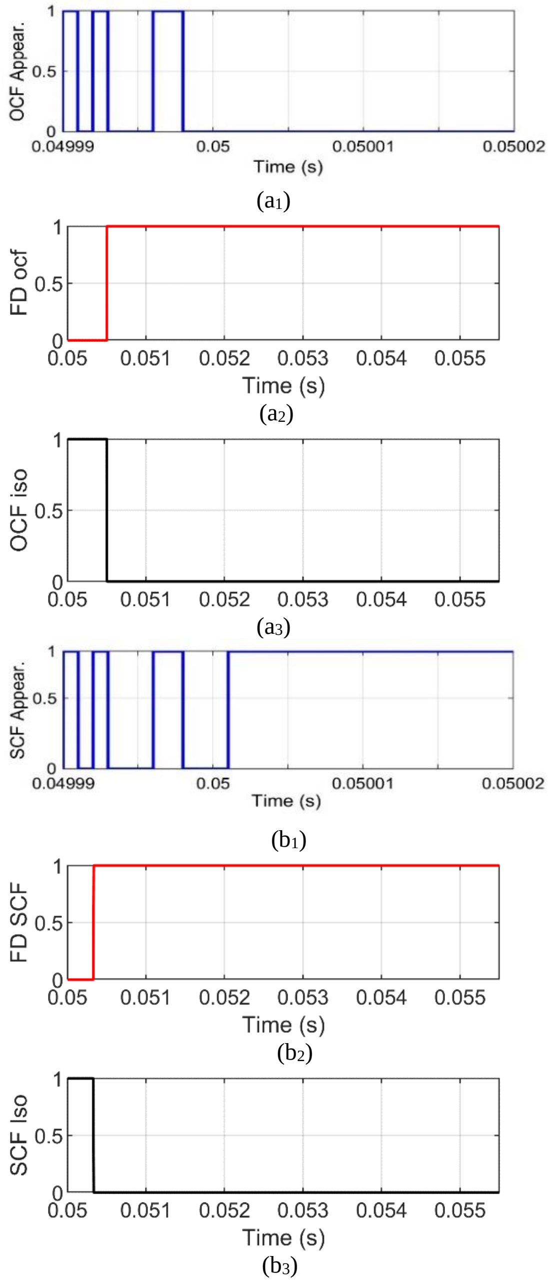

Fig. 19. Faults identification and isolation times of: a1) OCF appearance, a2) OCF detection, a3) OCF isolation, b1) SCF appearance, b2) SCF detection, b3) SCF isolation

5. CONCLUSIONS

This paper presents a new approach for detecting and isolating open-circuit faults (OCFs) and short-circuit faults (SCFs) in DC-DC boost converters. The primary objective of this study was to propose a fault diagnosis method for the investigated converter. The adaptive threshold-based fault diagnosis method offered the advantage of reducing the false alarm rate by making the system less susceptible to variations in the power supply of the IGBT. Based on the obtained results, it was demonstrated that the proposed technique is capable of detecting and identifying open-circuit (OC) and short-circuit (SC) faults in the converter. Moreover, the method effectively isolates these faults, ensuring the protection of the converter from potential damage. The adaptive threshold-based method proved to be fast and efficient in fault diagnosis, preventing further damage to the converter and minimizing the impact on global system operation. Furthermore, the results obtained from implementing the sliding mode control demonstrated its effectiveness and advantages in enhancing the performance of DC-DC boost converters. The controller exhibited stable and robust performance, reduced static error, and improved response time compared to the PI controller, making it a valuable control strategy for improving the overall performance and reliability of the DC-DC converters.

Following a successful fault diagnosis, selecting an appropriate fault-tolerant control strategy became critical. Fault-tolerant control plays a significant role in ensuring the reliability and robustness of power systems involving DC-DC converters. It involved designing control strategies that could detect and respond to faults in the power converter, enabling the system to continue operation and take appropriate actions to mitigate the effects of the fault. We can recommend various fault-tolerant control strategies, like redundancy-based control, to ensure system operation even in the presence of faults. For example, we could add redundant power switches or control modules to provide backup functionality. Another recommended strategy is reconfiguration, where the control system modifies control parameters and changes the control structure in real-time to adapt to the fault conditions. Future research will focus on evaluating these fault-tolerant control strategies experimentally.

Source of funding: *This research received no external funding.*

Author contributions: *research concept and design, F.K, A.A, S.F; Collection and/or assembly of data, A.A, F.K; Data analysis and interpretation, F.K, A.A, H.A; Writing the article, F.K, A.A, M.Z.D; Critical revision of the article, F.K, A.A, M.Z.D; Final approval of the article, A.A, S.F, H.A.*

Declaration of competing interest: *The authors declare that they have no known competing financial interests or personal relationships that could have appeared to influence the work reported in this paper.*

REFERENCES

1. Gehan O, Pigeon E, Menard T, Pouliquen M, Gualous H, Slamani Y. A Nonlinear state feedback for DC/DC boost converters. Journal of Dynamic Systems, Measurement, and Control 2017; 139(1): 011010. https://doi.org/10.1115/1.4034602.
2. Mansour AS, Zaky MS. A new extended single-switch high gain DC–DC boost converter for renewable energy applications. Scientific Reports 2023; 13(1): 264. https://doi.org/10.1038/s41598-022-26660-7.
3. Adnan MF, Oninda MAM, Nishat MM, Islam N. Design and simulation of a DC - DC boost converter with pid controller for enhanced performance. International Journal of Engineering Research and 2017; V6(09): IJERTV6IS090029. https://doi.org/10.17577/IJERTV6IS090029.
4. Pandey A, Borkar R, Kumbhar S, Ghunke P, Jain P. Comparison of power electronic converters with sliding mode control and open loop control. 2020 International Conference on Convergence to Digital World - Quo Vadis (ICCDW) 2020; 1–5. https://doi.org/10.1109/ICCDW45521.2020.9318726.
5. Raviraj VSC, Sen PC. Comparative study of proportional-integral, sliding mode, and fuzzy logic controllers for power converters. IEEE Transactions on Industry Applications 1997; 33(2): 518–24. https://doi.org/10.1109/28.568018.
6. Pei X, Nie S, Kang Y. Switch short-circuit fault diagnosis and remedial strategy for full-bridge DC–DC converters. IEEE Transactions on Power Electronics 2015; 30(2): 996–1004. https://doi.org/10.1109/TPEL.2014.2310201.
7. Yahyaoui R, De Bernardinis A, Gaillard A, Hissel D. Switch short-circuit fault detection algorithm based on drain-to-source voltage monitoring for a fault tolerant DC/DC converter. IECON 2016 - 42nd Annual Conference of the IEEE Industrial Electronics Society 2016; 2212–7. https://doi.org/10.1109/IECON.2016.7793949.
8. Kumar GK, Elangovan D. Review on fault-diagnosis and fault-tolerance for DC–DC converters. IET Power Electronics 2020; 13(1): 1–13. https://doi.org/10.1049/iet-pel.2019.0672.
9. Bento F, Cardoso AJM. A comprehensive survey on fault diagnosis and fault tolerance of DC-DC converters. Chinese Journal of Electrical Engineering 2018; 4(3): 1–12. https://doi.org/10.23919/CJEE.2018.8471284.
10. Givi H, Farjah E, Ghanbari T. Switch and diode fault diagnosis in nonisolated DC–DC converters using diode voltage signature. IEEE Transactions on Industrial Electronics 2018; 65(2): 1606–15. https://doi.org/10.1109/TIE.2017.2733486.
11. Jamshidpour E, Poure P, Saadate S. Common switch fault diagnosis for two-stage DC-DC converters used in energy harvesting applications. Electronics 2019;8(3):293. https://doi.org/10.3390/electronics8030293.
12. Jamshidpour E, Poure P, Saadate S. Photovoltaic systems reliability improvement by real-time FPGA-based switch failure diagnosis and fault-tolerant DC–DC converter. IEEE Transactions on Industrial Electronics 2015; 62(11): 7247–55. https://doi.org/10.1109/TIE.2015.2421880.
13. Chen Y, Nie S, Pei X, Kang Y. State monitoring and fault diagnosis of the PWM converter using the magnetic field near the inductor components. 2010 IEEE Energy Conversion Congress and Exposition 2010; 1901–7. https://doi.org/10.1109/ECCE.2010.5618317.
14. Chen Y, Pei X, Nie S, Kang Y. Monitoring and diagnosis for the DC–DC converter using the magnetic near field waveform. IEEE Transactions on Industrial Electronics 2011; 58(5): 1634–47. https://doi.org/10.1109/TIE.2010.2051939.
15. Jamshidpour E, Poure P, Gholipour E, Saadate S. Single-Switch DC–DC converter with fault-tolerant

capability under open- and short-circuit switch failures. IEEE Transactions on Power Electronics 2015; 30(5): 2703–12. https://doi.org/10.1109/TPEL.2014.2342878.
16. Jamshidpour E, Poure P, Saadate S. Switch failure diagnosis based on inductor current observation for boost converters. International Journal of Electronics 2016:1–12. https://doi.org/10.1080/00207217.2016.1138243.
17. Espinoza Trejo DR, Taheri S, Pecina Sánchez JA. Switch fault diagnosis for boost DC–DC converters in photovoltaic MPPT systems by using high-gain observers. IET Power Electronics 2019; 12(11): 2793–801. https://doi.org/10.1049/iet-pel.2018.6287.
18. Xu L, Ma R, Xie R, Xu J, Huangfu Y, Gao F. Open-circuit switch fault diagnosis and fault- tolerant control for output-series interleaved boost DC–DC converter. IEEE Transactions on Transportation Electrification 2021; 7(4): 2054–66. https://doi.org/10.1109/TTE.2021.3083811.
19. Reyes-Cruz D, Martinez-Rodriguez PR, Langarica-Cordoba D, Vazquez-Guzman G, Sosa-Zuñiga JM, Ramirez-Rivera VM. Control strategies and experimental validation for high-gain non-isolated double inductor boost converter. Engineering Science and Technology, an International Journal 2023; 37: 101294. https://doi.org/10.1016/j.jestch.2022.101294.
20. Guldemir H. Sliding Mode Control of Dc-Dc Boost Converter. Journal of Applied Sciences 2005; 5(3): 588–92. https://doi.org/10.3923/jas.2005.588.592.
21. Sun J. Pulse-Width modulation. Dynamics and CONTROL OF SWITCHED ELECTRONIC SYSTEMS 2012; 25–61. https://doi.org/10.1007/978-1-4471-2885-4_2.
22. Taniguchi K, Ogino Y, Irie H. PWM technique for power MOSFET inverter. IEEE Transactions on Power Electronics 1988; 3(3): 328–34. https://doi.org/10.1109/63.17951.
23. Hussein AI, Shigdar B, Almatrafi L, Alaidroos B, Alsharif F, Aly RHM. Design of a DC/DC converter with a PID controller and backpropagation neural network for electric vehicles. 2023 20th Learning and Technology Conference (L&T) 2023; 128–33. https://doi.org/10.1109/LT58159.2023.10092291.
24. Dave MR. Analysis of boost converter using PI control algorithms. 2012
25. Tan SC, Lai YM, Tse CK. Implementation of pulse-width-modulation based sliding mode controller for boost converters. IEEE Power Electronics Letters 2005; 3(4): 130–5. https://doi.org/10.1109/LPEL.2005.863269.
26. Hongmei Li, Xiao Ye. Sliding-mode PID control of DC-DC converter. 2010 5th IEEE Conference on Industrial Electronics and Applications 2010; 730–4. https://doi.org/10.1109/ICIEA.2010.5516952.
27. Komurcugil H, Biricik S, Bayhan S, Zhang Z. Sliding mode control: Overview of its applications in power converters. IEEE Industrial Electronics Magazine 2021; 15(1): 40–9. https://doi.org/10.1109/MIE.2020.2986165.
28. Wu L, Liu J, Vazquez S, Mazumder SK. Sliding mode control in power converters and drives: A Review. IEEE/CAA Journal of Automatica Sinica 2022; 9(3): 392–406. https://doi.org/10.1109/JAS.2021.1004380.
29. Chen L, Zhao X, Tang SX. Online fault diagnosis method for high-performance converters using inductor voltage polar signatures. IEEE Access 2020; 8: 179778–88. https://doi.org/10.1109/ACCESS.2020.3024549.
30. Abderrezak A, Madjid K. Sensor fault detection, localization, and system reconfiguration with a sliding mode observer and adaptive threshold of PMSM. Journal of Power Electronics 2016; 16(3): 1012–24. https://doi.org/10.6113/JPE.2016.16.3.1012.
31. Aktas M, Aygun H. Comparison of DC link current and stator phase current in inverter switching faults detection of PMSM drives in HEVs. Engineering Science and Technology, an International Journal 2018; 21(4): 664–71. https://doi.org/10.1016/j.jestch.2018.06.002.
32. Han J, Zhang Z, Lai Q, Yin X. Open-circuit fault characteristics and location methods of switch elements for cascaded power electronic transformers. IEEE Transactions on Power Delivery 2022; 37(2): 1017–26. https://doi.org/10.1109/TPWRD.2021.3075487.
33. Bento F, Marques Cardoso AJ. Fault diagnosis in DC-DC converters using a time-domain analysis of the reference current error. IECON 2017 - 43rd Annual Conference of the IEEE Industrial Electronics Society 2017; 5060–5. https://doi.org/10.1109/IECON.2017.8216874.
34. Rojas F, Jerez C, Hackl CM, Kalmbach O, Pereda J, Lillo J. Faults in modular multilevel cascade converters–Part II: fault tolerance, fault detection and diagnosis, and system reconfiguration. IEEE Open Journal of the Industrial Electronics Society 2022; 3: 594–614. https://doi.org/10.1109/OJIES.2022.3213508.

Fatma KHATER
was born in Saida, Algeria. She holds a Master's degree in Automation from the Faculty of Hydrocarbons and Chemistry, University M'hamed Boughara of Boumerdes, Algeria. Currently, she prepares his Phd thesis in automatic control, at Applied Automatic Control Laboratory (LAA), Faculty of Hydrocarbons and Chemistry, M'hamed Bougara University of Boumerdes. She is currently interested in research on power converters control and fault diagnosis.
e-mail: f.khater@univ-boumerdes.dz

Abderrezak AIBECHE
was born in Bouhatem-Mila-Algeria. He received his B.Sc., M.Sc., and PhD degrees in Electrical Engineering from the University M'Hamed Bougara of Boumerdes, Faculty of Hydrocarbons and Chemistry, in 2001, 2009, and 2016, respectively. He has been associate professor with the Department of Electrical Systems Engineering in the University M'Hamed Bougara of Boumerdes, Faculty of Technology, since January 2013, and he is a member of the Scientific Committee of the Department and he is a research team member on «Control of complex dynamical systems» at Applied Automation

Laboratory, Boumerdes, since 2005. Currently, his research interests include power conversion techniques, control of power converters, sensorless control of AC drives, fault diagnosis, fault-tolerant control of power systems, and renewable energy.
e-mail: aibeche_umbb@univ-boumerdes.dz

Sid Ali FELLAG, born in 1972 in Algeria, completed his school studies there. He received his master and PhD degrees from the technical university of Tashkent respectively in 1995 and 2000, the PhD dissertation was on "The electromagnetic shaft system designed for long conveyors" under supervision of professor Usmankhodjaev: the inventor of electromagnetic shaft (a modified version of electrical shaft). From 2000 till now he is a full professor at Boumerdes university in Algeria.
e-mail: s.fellag@univ-boumerdes.dz

Mohamed Zinelabidine DOGHMANE is a highly experienced petroleum expert with over ten years of experience working with the National Oil Company of Algeria (SONATRACH) and seven years of teaching at the University of Boumerdes. He has worked with a wide variety of applied automation and petroleum reservoirs, including sedimentary, carbonate, unconventional, tight, and low-resistivity reservoirs in Algeria. Mohamed has an advanced academic background, having published more than 85 research papers and proceedings, wrote two books and supervising 10 PhD theses at the University of Boumerdes, Algeria. He is a reviewer for many well-reputed journals, and he is a member of the scientific committees of many international conferences. He is now focused on converting his industry knowledge into a PhD thesis, research papers, patents, and books. With his wealth of knowledge and experience in the field of reservoir engineering and applied automation, Mohamed's work promises to be an invaluable resource for researchers, engineers, and practitioners in the field.
e-mail: m.doghmene@univ-boumerdes.dz

Hamza AKROUM is an associate professor in the Faculty of Technology at M'Hamed Bougara University, Boumerdes, Algeria. He received his Engineering and Magister degree in electronics engineering both from the National Polytechnic School of Algiers. He received his Doctorate-Sciences degree in automatic from Hydrocarbons and Chemistry Faculty at Boumerdes University, Algeria. He has been working at the Algerian nuclear research center of Birine in instrumentation department (CRNB/DEDIN). He is a research group member on «Control of complex dynamical systems» at Applied Automatic Control Laboratory, Boumerdes University. His research interest includes optimization applied to control drives, modeling and control of dynamic nonlinear systems, power converters, sensorless control of AC drives and Renewable energy.
e-mail: akroum@univ-boumerdes.dz